4

Bonds and Energy Bands

CHAPTER PREVIEW

Bonding in ceramic materials may be quite complicated. It will be primarily covalent and/or ionic, but it may also have a metallic component, a van der Waals component, etc. In this chapter we will review the basic types of primary and secondary bonds and see how they apply to ceramics. We will also review the concept of energy bands, which we use in discussing electrical properties later. The purpose of this chapter is to review the concepts that we will use throughout the text. If it is not a review for you, suggestions are given for suitable texts that will give you the details. Important topics include the type of bonding, the origin of hybridization, mixed bonding, and energy bands.

4.1 TYPES OF INTERATOMIC BOND

We can divide interatomic bonds into two categories:

- Primary (strong) bonds
- Secondary (weak) bonds

The types of primary and secondary bonds and their energy ranges are given in Table 4.1. In the next few sections we will briefly review the general characteristics of these bonds.

All interatomic forces are electrostatic in origin. The simplest expression for the bond energy is

$$E = -\frac{A}{r^n} + \frac{B}{r^m} \tag{4.1}$$

where r is the interatomic distance and A, B, n, and m are constants characteristic of the type of bonding. The first term is the attractive component the second is due to repulsion. Only when $m > n$ will a minimum (equilibrium) value of E be possible. Equation 4.1 indicates that attractive forces predominate when atoms are far apart and repulsive interactions predominate when the atoms are close together. The bond–energy curve can be plotted as shown in Figure 4.1a. When the energy is a minimum the atoms are at their equilibrium separation ($r = r_0$); the lowest energy state defines the equilibrium condition. In discussing ceramics, we usually think of the material in terms of ions; ions with the same sign always repel one another due to the Coulomb force.

If we differentiate Eq. 4.1 with respect to r, we obtain an equation that describes the resultant force F between a pair of atoms

$$F = \frac{\mathrm{d}E}{\mathrm{d}r} = \frac{nA}{r^{n+1}} - \frac{mB}{r^{m+1}} \tag{4.2}$$

The force will be zero at the equilibrium separation.

The sign conventions for force: In Figure 4.1a the force is attractive when F is positive. This is the usual convention in materials science (and in Newton's law of universal gravitation). The force is attractive if $A > 0$ and negative if $A < 0$. Beware: in electrostatics, the convention is that a negative force is attractive.

4.2 YOUNG'S MODULUS

We can change the equilibrium spacing (r_0) of the atoms in a solid by applying a force. We can push the atoms closer together (compression), $r < r_0$, or pull them further apart (tension), $r > r_0$. Young's modulus ($\mathcal{E}$) is a measure of the resistance to small changes in the separation of adjacent atoms (*modulus* is Latin for "a small measure"). It is the same for both tension and compression.

Young's modulus is related to the interatomic bonding forces and, as you might expect, its magnitude depends on the slope of the force–distance curve at r_0.

Close to r_0 the force–distance curve approximates a tangent; when the applied forces are small the displacement of the atoms is small and proportional to the force. We can define the stiffness of the bond, S_0, as the slope of this line:

$$S_0 = \left(\frac{\mathrm{d}F}{\mathrm{d}r}\right)_{r=r_0} = \left(\frac{\mathrm{d}^2E}{\mathrm{d}r^2}\right)_{r=r_0} \tag{4.3}$$

TABLE 4.1 Typical Bond Strengths

Type of bond	*Bond energy (kJ/mol)*
Ionic	50–1000
Covalent	200–1000
Metallic	50–1000
van der Waals	0.1–10
Hydrogen	10–40

The stiffness is analogous to the spring constant or elastic force constant of a spring and is the physical origin of Hooke's law. Close to r_0 we can assume that the force between two atoms that have been stretched apart a small distance r is

$$F = S_0(r - r_0) \tag{4.4}$$

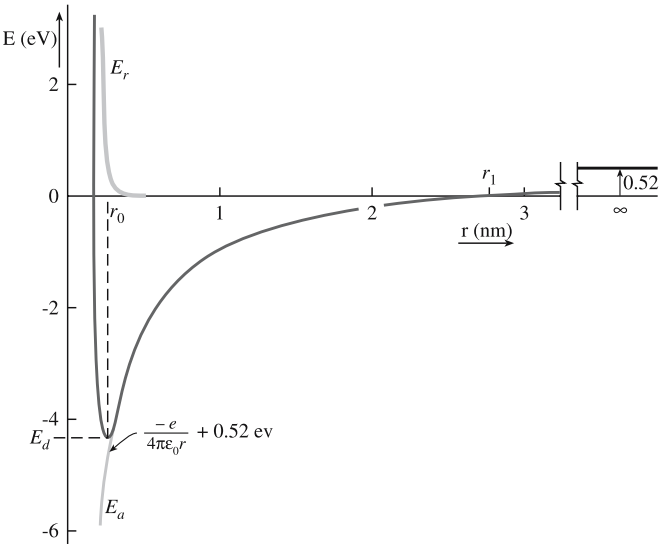

(A)

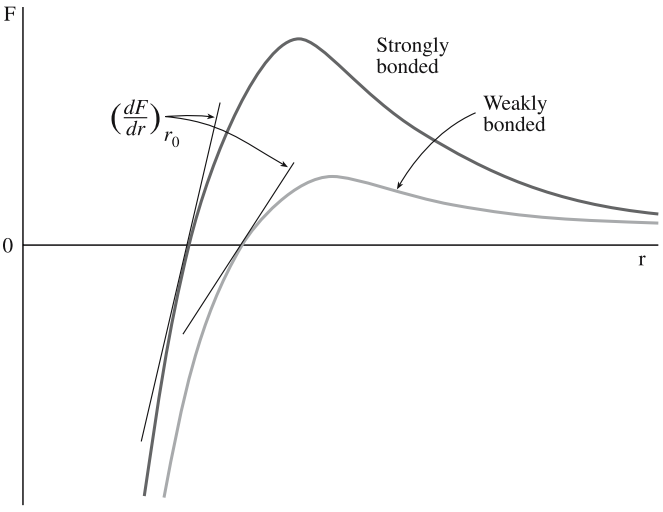

(B)

FIGURE 4.1 (a) Bond-energy curve for KCl. At infinite separation, the energy is that required to form K^+ and Cl^- from the corresponding atoms. (b) Force-distance curves for two materials: one where the bonding is strong and one where it is weak.

If we consider pulling two planes of atoms apart then the total force per unit area can be obtained by dividing F by r_0^2

$$\frac{F}{r_0^2} = \sigma = \frac{S_0(r - r_0)}{r_0^2} = \frac{S_0}{r_0}\left(\frac{r - r_0}{r_0}\right) = \mathcal{E}\varepsilon \tag{4.5}$$

where σ and ε should be familiar to you already, they are stress and strain, respectively. Moduli obtained from this approach are approximate because they relate to two atoms only, ignoring the effects of neighboring atoms. (Although we only discussed Young's modulus here the conclusions are applicable to the other elastic moduli we describe in Chapter 16.) As the interatomic spacing, and in some cases the bonding, varies with direction in a single crystal, Young's modulus is dependent upon the direction of stress in relation to the crystal axes. Single crystals are elastically anisotropic.

Figure 4.1b shows force–distance plots for two materials; one having weakly bonded atoms and the other having strongly bonded atoms. With reference to bond–energy curves a material with a high modulus will have a narrow, steep potential energy well; a broad, shallow energy well would be characteristic of a low modulus. Table 4.2 lists values of Young's moduli for different materials as a function of melting temperature. You can see the general trend: the higher the melting temperature, the higher the modulus. Melting temperatures are also indicative of bond strengths, which are determined mainly by the depth of the energy well. The modulus is determined by the curvature at the bottom of the well. It is this difference that accounts for deviations from the general trend.

As the temperature of a material is increased it is generally found that Young's modulus slowly decreases as shown for single-crystal aluminum oxide (corundum) in

TABLE 4.2 Young's Moduli as a Function of Melting Temperature

Compound	*Average Young's modulus (GPa)*	*Melting temperature, (°C)*
Titanium carbide	310	3180
Tungsten	414	2996
Silicon carbide	345	Sublimes > 2800
Periclase (MgO)	207	2800
Beryllia (BeO)	310	2585
Spinel ($MgAl_2O_4$)	241	2160
Corundum (Al_2O_3)	366	2050
Iron	207	1539
Copper	110	1083
Halite (NaCl)	34	801
Aluminum	69	660
Magnesium	41	650
Polystyrene	2.8	<300
Nylon	2.8	<300
Rubber	0.07	<300

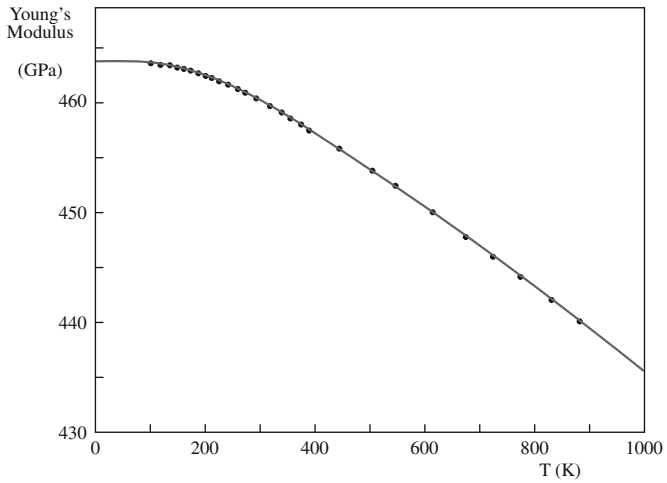

FIGURE 4.2 Temperature dependence of Young's modulus for corundum.

Figure 4.2. As we approach absolute zero, the slope of the curve approaches zero as required by the third law of thermodynamics. (The entropy of any pure substance in complete internal equilibrium is zero.) An empirical relationship that fits the data for several ceramics is

$$\mathcal{E} = \mathcal{E}_0 - bT\exp\left(\frac{-T_0}{T}\right) \tag{4.6}$$

$\mathcal{E}_0$ is Young's modulus at absolute zero and b and T_0 are empirical constants; T_0 is about half the Debye temperature. (The Debye temperature is the temperature at which the elastic vibration frequency of the atoms in a solid is the maximum.) As the temperature is increased the separation between the atoms is increased and the force necessary for further increases is slightly decreased.

For polycrystalline ceramics there is an additional effect due to grain boundaries. At high temperatures there is a rapid decrease in the measured values of Young's moduli as shown in Figure 4.3. This has been attributed to nonelastic effects such as grain boundary sliding and grain boundary softening. So Young's modulus of a bulk ceramic is continuing to change as described by Eq. 4.6, but we are measuring changes due to the grain boundaries. The importance of grain boundaries in the mechanical behavior of ceramics will become very apparent in later chapters.

4.3 IONIC BONDING

In a pure ionic bond there is complete transfer of electrons from one atom to another. Pure ionic compounds do not exist. Although compounds such as NaCl and LiF are often thought of as being ionic, in general, all such "ionic" solids have a covalent component.

The requirement for ionic bonding is that the ionization energy to form the cation and the electron affinity to form the anion must both favor it energetically. The formation of isolated ions from isolated atoms requires energy and, thus, the formation of the pair of ions would not produce a stable situation. However, the pair of ions will have a strong mutual attraction that leads to a strong binding in the molecule. Because the Coulomb force is strong and long range, many ionic compounds have high melting and high boiling temperatures. Ionic bonds do not favor particular directions. This is very different from covalent bonding.

Energy of an Ion Pair

Before considering a lattice of ions, we will consider a single pair of oppositely charged ions separated by a distance r. The electrostatic attractive energy E is

$$E = -\frac{|Z_M||Z_X|e^2}{(4\pi\varepsilon_0 r)} \tag{4.7}$$

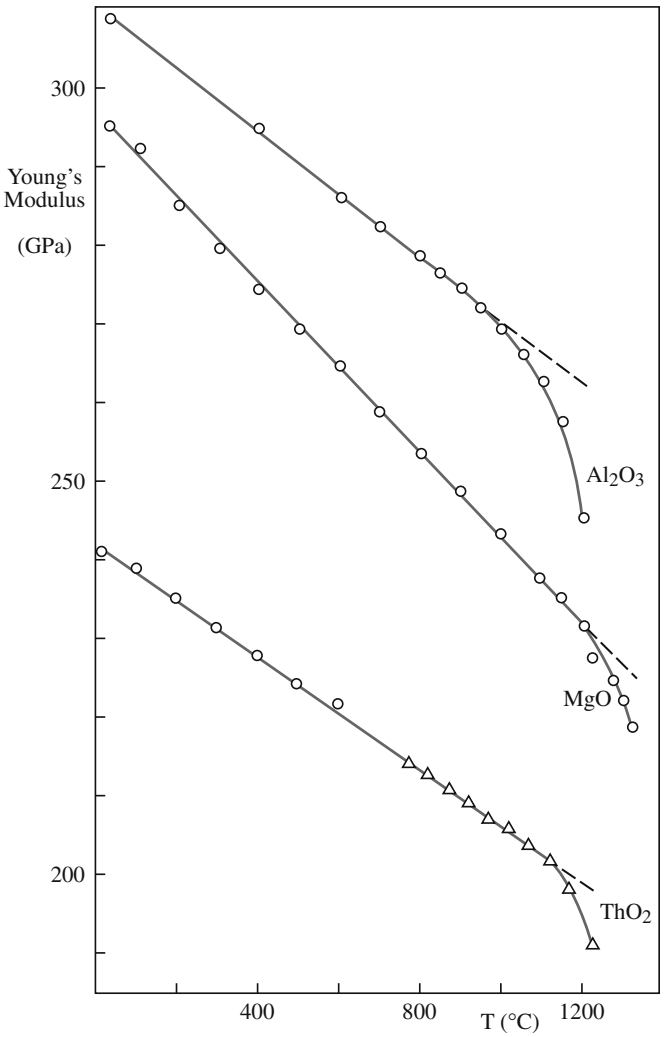

FIGURE 4.3 Temperature dependence of Young's modulus of several polycrystalline ceramics.

Z_M and Z_X are the charges on the cation and anion, respectively. The negative sign in Eq. 4.7 means that as r becomes smaller, the energy becomes increasingly more negative. To obtain equilibrium separation there must be repulsion to balance the attraction. Strong repulsive forces arise when the full electron orbitals of both ions overlap, because some electrons must then go into higher energy states in accordance with the Pauli exclusion principle. The repulsion energy rises rapidly with decreasing distance between the ions.

The repulsive energy is often given by an equation of the form

$$E_r = \frac{B}{r^n} \tag{4.8}$$

B is a constant and n is known as the Born exponent. Information about the Born exponent may be obtained from compressibility data since we are measuring the resistance of the ions to be closer together than r_0. The Born exponent depends on the type of ion involved. Larger ions have higher electron densities and hence larger values of n (Table 4.3).

The total energy of the ion pair is given by summing Eqs. 4.7 and 4.8

$$E = -\frac{|Z_M||Z_X|e^2}{(4\pi\varepsilon_0 r)} + \frac{B}{r^n} \tag{4.9}$$

The inset in Figure 4.1a shows how when r is large the bond energy is >0, because of the net energy involved in forming the ion pair.

Madelung Constant

In a crystal lattice, all the ions will interact. The interaction between ions with opposite charge will be attractive, but will be repulsive between ions of like charge. The summation of all these interactions is known as the Madelung constant, $\mathcal{A}$ (Madelung, 1918). The energy per ion pair in the crystal is then

$$E = -\frac{\mathcal{A}|Z_M||Z_X|e^2}{(4\pi\varepsilon_0 r_0)} \tag{4.10}$$

The Madelung constant is defined as the ratio of the Coulomb energy of an ion pair in a crystal to the Coulomb energy of an isolated ion pair at the same separation (the equilibrium separation of the ions in the crystal not in an isolated pair).

$$\mathcal{A} = \sum_i -\frac{Z_i Z_j}{|Z_1||Z_2| r_{ij}} \tag{4.11}$$

The distance r_{ij} is the separation between ions at equilibrium.

In three dimensions the series presents greater difficulty than the linear example. It is not possible to write down the successive terms by quick inspection. More importantly, the series converges slowly and keeps reversing in sign so you have to consider the whole infinite crystal.

An approach we can use to obtain $\mathcal{A}$ for a three-dimensional crystal structure is illustrated for NaCl (Figure 4.5). We want to consider the interactions between the central cation and all the other ions in the cell. Due to electroneutrality requirements in the unit cell, ions located on the cube faces count 1/2, those on the cell edges count 1/4, and the corner ions count 1/8. (This is the same approach that you use when determining the number of atoms per cell.)

Using Eq. 4.11 we obtain

$$\mathcal{A} = -(6/2)(-1)/1 - (12/4)(1)/\sqrt{2} - (8/8)(-1)/\sqrt{3}$$

Hence

$$\mathcal{A} = 3 - 2.1212 + 0.5774 = 1.456$$

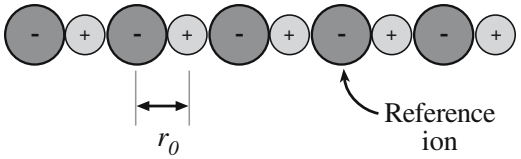

FIGURE 4.4 Linear array of ions of alternate sign separated by r_0.

MADELUNG CONSTANT FOR LINEAR ARRAY

For the infinite linear array of ions shown in Figure 4.4 we obtain

$$\mathcal{A} = 2[1 - 1/2 + 1/3 - 1/4 + \ldots]$$

The factor 2 occurs because there are two ions, one to the right and one to the left of our reference ion, at equal distances r_{ij}. We sum this series using the expansion

$$\ln(1 + x) = x - x^2/2 + x^3/3 - x^4/4 + \ldots$$

Thus the linear Madelung constant

$$\mathcal{A} = 2\ln 2.$$

TABLE 4.3 Values of the Born Exponent, *n*

Ion configuration	*n*
He	5
Ne	7
Ar, Cu^+	9
Kr, Ag^+	10
Xe, Au^+	12

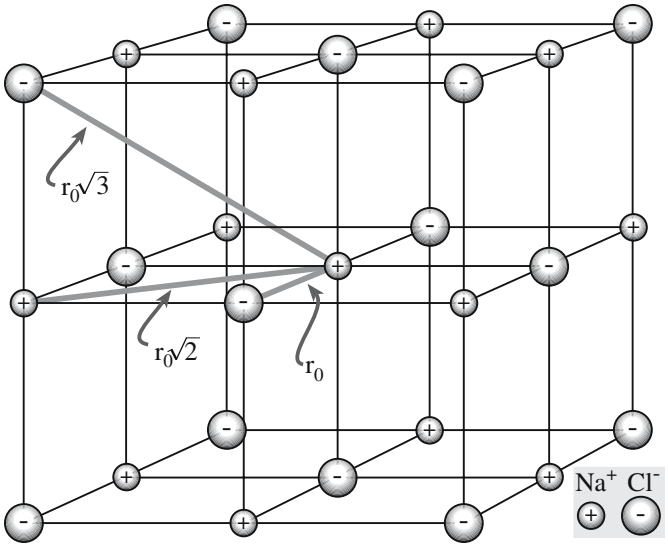

FIGURE 4.5 NaCl structure showing distances between ions in multiples of r_0.

If we consider a larger cell size the value we obtain for the Madelung constant is closer to that determined for the NaCl structure using computer calculations. Doubling the length of the cell edge gives $\mathcal{A} = 1.75$. These simple calculations are a little misleading because the sum is really infinite. There are two important points:

- $\mathcal{A}$ is well defined for a particular crystal structure, it is usually ~2.
- $\mathcal{A}$ is unique for a particular crystal structure and is the same for NaCl and MgO.

Table 4.4 lists Madelung constants for some common crystal structures. The value of the Madelung constant is determined only by the geometry of the lattice and is independent of the ionic radius and charge. Unfortunately, some tables incorporate ionic charge, so care is necessary when looking up and comparing values. For example, the Madelung constant for fluorite may be given as 5.038 and that of Al_2O_3 as 25.031; the constant for MgO may then be given as different from that for NaCl.

Table 4.4 confirms that the value of the Madelung constant for all these different crystal structures is greater than 1. The implication is that the crystal is more stable than an isolated ion pair. The fact that the Madelung constant for the NaCl structure, which has six nearest neighbors, is close to the Madelung constant of the CsCl structure, which has eight nearest neighbors, indicates that

- The number of neighbors does not significantly influence the lattice energy.
- The Coulomb energy does not depend on the type of crystal structure.

TABLE 4.4 Madelung Constants of Some Common Crystal Structures

Structure	*Coordination number*	*Geometric factor, $\mathcal{A}$*
Sodium chloride	6:6	1.74756
Cesium chloride	8:8	1.76267
Zinc blende	4:4	1.63806
Wurtzite	4:4	1.64132
Fluorite	8:4	2.51939
Rutile	6:3	2.408[a]
Corundum	6:4	4.1719[a]

In Chapter 5 we will see that packing is the most important consideration in determining the structure adopted by predominantly ionically bonded crystals. The difference in $\mathcal{A}$ between some crystal structures is very small. In such cases, for example, the zinc blende and wurtzite structures (named after the two crystalline forms of ZnS), the difference in the resulting electrostatic energy is small. For zinc blende and wurtzite it is ~0.2%. When the energy difference between structure types of the same stoichiometry is small, we often encounter polymorphism: the compound can form with more than one structure. We will examine this useful complication in Chapter 7.

Lattice Energy

With knowledge of the Madelung constant we write the total energy for 1 mol of the crystal lattice containing an Avogadro's number (N) of ion pairs:

$$E = -\frac{\mathcal{A}N|Z_M||Z_X|e^2}{(4\pi\varepsilon_0 r)} + \frac{NB}{r^n} \tag{4.12}$$

The minimum energy, E_0, at r_0 is obtained by differentiating Eq. 4.12 with respect to r:

$$\frac{dE}{dr} = 0 = \frac{\mathcal{A}N|Z_M||Z_X|e^2}{(4\pi\varepsilon_0 r_0^2)} - \frac{nBN}{r^{n+1}}$$

The constant B is then

$$B = \frac{\mathcal{A}N|Z_M||Z_X|e^2 r_0^{n-1}}{4\pi\varepsilon_0}$$

Rewriting Eq. 4.12 gives the Born–Landé equation, which is quite successful in predicting accurate values of the lattice energy of an ionic compound:

$$E_0 = -\frac{\mathcal{A}N|Z_M||Z_X|e^2}{4\pi\varepsilon_0 r_0}\left(1 - \frac{1}{n}\right) \tag{4.13}$$

It requires only knowledge of the crystal structure (in order to choose $\mathcal{A}$ correctly) and r_0. Both parameters are readily available from X-ray diffraction data.

As an example of using Eq. 4.13 we will calculate the value of E_0 for MgO. We need to substitute the following values:

$\mathcal{A}$ = 1.748 (from Table 4.4)
n = 8 (an average value based on Table 4.3)
r_0 = 210 pm (from X-ray diffraction data)

This gives $E_0 = -4046.8$ kJ/mol.

The terms in Eq. 4.1 are modified in other models since it would be surprising for one value of n to fit all atoms when we have no physical justification for any particular number. For example, the repulsion term may be represented by

$$E_r = be^{-(r/\rho)} \tag{4.14}$$

Where b and ρ are constants determined from compressibility measurements. This gives the Born–Mayer equation (Born and Mayer, 1932) for lattice energy:

$$E_0 = -\frac{\mathcal{A}N|Z_M||Z_X|e^2}{4\pi\varepsilon_0 r_0}\left(1-\frac{\rho}{r_0}\right) \tag{4.15}$$

The Born–Mayer equation emphasizes the fact that Eq. 4.1 is designed only to match the observed phenomenon. It is not a fundamental "truth" like the Coulomb interaction.

The Born–Haber Cycle

The Born–Haber (Born, 1919; Haber, 1919) cycle shows the relationship between lattice energy and other thermodynamic quantities. It also allows the lattice energy to be calculated. The background of the Born–Haber cycle is Hess's law, which states that the enthalpy of a reaction is the same whether the reaction proceeds in one or several steps. The Born–Haber cycle for the formation of an ionic compound is shown in Figure 4.6. It is a necessary condition that

$$\Delta H_f = \Delta H_{AM} + \Delta H_{AX} + \Delta H_{IE} + \Delta H_{EA} + E \tag{4.16}$$

or in terms of the lattice energy

$$E = \Delta H_f - \Delta H_{AM} - \Delta H_{AX} - \Delta H_{IE} - \Delta H_{EA} \tag{4.17}$$

ΔH_{AM} and ΔH_{AX} are the enthalpies of atomization of the metal and the nonmetal, respectively.

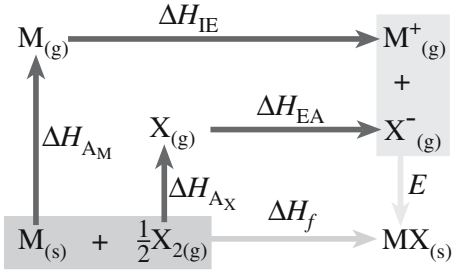

FIGURE 4.6 The Born–Haber cycle.

TABLE 4.5 Lattice Energies of Some Alkali and Alkaline Earth Metal Halides at 0 K (kJ/mol)

Compound	*Born–Haber cycle*	*Born–Landé equation*
NaF	−910	−904
NaCl	−772	−757
NaBr	−736	−720
NaI	−701	−674
KCl	−704	−690
KI	−646	−623
CsF	−741	−724
CsCl	−652	−623
CsI	−611	−569
MgF_2	−2922	−2883
CaF_2	−2597	−2594

For gaseous diatomic molecules ΔH_A is the enthalpy of dissociation (bond energy plus RT) of the diatomic molecule. For metals that vaporize to form monatomic gases ΔH_A is identical to the enthalpy of sublimation. If a diatomic molecule M_2 sublimes, then the dissociation enthalpy of the reaction ($M_2 \rightarrow 2M$) must also be included. As defined earlier, E is the lattice energy of the crystal and represents the heat of formation per mole of a crystal MX from $M^+_{(g)}$ and $X^-_{(g)}$.

As an example of using the Born–Haber cycle we will calculate the lattice energy of MgO. The values of the various thermodynamic parameters can be found in Kubaschewski *et al.* (1993), Johnson (1982), and in the NIST-JANAF tables (Chase, 1998).

For MgO:

ΔH_f −601.7 kJ/mol
ΔH_{AM} 147.7 kJ/mol
ΔH_{AX} 249 kJ/mol [the actual value for the dissociation enthalpy is 498 kJ/mol, but we need to take half this value because we are considering the reaction ½O_2 (g) → O (g)]
ΔH_{IE} 2188 kJ/mol
ΔH_{EA} −638 kJ/mol

By substitution into Eq. 4.17 we get E = –2548.4 kJ/mol.

If we compare this value with that calculated using the Born–Landé equation we see that they are quite different. The Born–Haber cycle gives a lattice energy about 60% higher than the Born–Landé value. The reason for this difference is that although we often regard MgO as essentially an ionic ceramic, it does have an appreciable covalent character. If similar calculations, using the Born–Landé equation and the Born–Haber cycle, are performed for NaCl or one of the other alkali halides the values obtained using the two methods agree to within 1% or 2% as shown in Table 4.5. The differences in the above calculations are sometimes used as a means of defining an ionic compound—if the results are similar, it must be ionic. Although this definition is not too useful within the context of ceramics, it does serve as an illustration that the bonding in most ceramics is not simply ionic.

Ionic Radii

We know from quantum mechanics that atoms and ions do not have precisely defined radii. However, the concept of an ion as a hard sphere with a fixed radius is very useful when predicting crystal structures. Experimental evidence shows that such a model has some justification: the model often "works." Nevertheless, always bear in mind that atoms and ions are not rigid spheres and their size will be affected by their local environment.

We cannot measure ionic radii directly. What we can measure rather easily, and with high accuracy using X-ray crystallography, in most crystals is r_0.

$$r_0 = r_M + r_X \tag{4.18}$$

r_M is the radius of the cation (usually a metal) and r_X is the radius of the anion.

To obtain ionic radii it is necessary to fix the radius of one of the ions in Eq. 4.18. Historically, the radius of the I^- ion was fixed and the other radii calculated with respect to it (Landé, 1920). Later, Pauling (1960) produced a consistent set of ionic radii that has been used widely for many years. Many mineralogists use Goldschmidt's values. The most comprehensive set of ionic radii is that compiled by Shannon and Prewitt (1969) and revised by Shannon (1976). Table 4.6 lists Shannon's ionic radii. Although there are several different tabulations they are, for the most part, internally consistent. So it is important to use radii from only one data set. Never mix values from different tabulations.

There are several important trends in the sizes of ions:

- The radii of ions within a group in the periodic table increase with increasing Z (this is for main group elements; the transition metals often behave differently).
- The radius of a cation is smaller than the corresponding atom.
- The radius of an anion is larger than the corresponding atom.
- In a particular row of the periodic table the anions are larger than the cations.

Using X-ray methods, it is possible to obtain accurate electron density maps for ionic crystals; NaCl and LiF are shown in Figure 4.7. It has been suggested that the

TABLE 4.6 Ionic Crystal Radii (in pm)

Coordination Number = 6

Ag^+	Al^{3+}	As^{5+}	Au^+	B^{3+}	Ba^{2+}	Be^{2+}	Bi^{3+}	Bi^{5+}	Br^-	C^{4+}	Ca^{2+}	Cd^{2+}
115	54	46	137	27	135	45	103	76	196	16	100	95
Ce^{4+}	Cl^-	Co^{2+}	Co^{3+}	Cr^{2+}	Cr^{3+}	Cr^{4+}	Cs^+	Cu^+	Cu^{2+}	Cu^{3+}	Dy^{3+}	Er^{3+}
87	181	75	55	80	62	55	167	77	73	54	91	89
Eu^{3+}	F^-	Fe^{2+}	Fe^{3+}	Ga^{3+}	Gd^{3+}	Ge^{4+}	Hf^{4+}	Hg^{2+}	Ho^{3+}	I^-	In^{3+}	K^+
95	133	78	65	62	94	53	71	102	90	220	80	138
La^{3+}	Li^+	Mg^{2+}	Mn^{2+}	Mn^{4+}	Mo^{3+}	Mo^{4+}	Mo^{6+}	N^{5+}	Na^+	Nb^{5+}	Nd^{3+}	Ni^{2+}
103	76	72	83	53	69	65	59	13	102	64	98	69
Ni^{3+}	O^{2-}	OH^-	P^{5+}	Pb^{2+}	Pb^{4+}	Rb^+	Ru^{4+}	S^{2-}	S^{6+}	Sb^{3+}	Sb^{5+}	Sc^{3+}
56	140	137	38	119	78	152	62	184	29	76	60	75
Se^{2-}	Se^{6+}	Si^{4+}	Sm^{3+}	Sn^{4+}	Sr^{2+}	Ta^{5+}	Te^{2-}	Te^{6+}	Th^{4+}	Ti^{2+}	Ti^{3+}	Ti^{4+}
198	42	40	96	69	118	64	221	56	94	86	67	61
Tl^+	Tl^{3+}	U^{4+}	U^{5+}	U^{6+}	V^{2+}	V^{5+}	W^{4+}	W^{6+}	Y^{3+}	Yb^{3+}	Zn^{2+}	Zr^{4+}
150	89	89	76	73	79	54	66	60	90	87	74	72

Coordination Number = 4

Ag^+	Al^{3+}	As^{5+}	B^{3+}	Be^{2+}	C^{4+}	Cd^{2+}	Co^{2+}	Cr^{4+}	Cu^+	Cu^{2+}	F^-	Fe^{2+}
100	39	34	11	27	15	78	58	41	60	57	131	63
Fe^{3+}	Ga^{3+}	Ge^{4+}	Hg^{2+}	In^{3+}	Li^+	Mg^{2+}	Mn^{2+}	Mn^{4+}	Na^+	Nb^{5+}	Ni^{2+}	O^{2-}
49	47	39	96	62	59	57	66	39	99	48	55	138
OH^-	P^{5+}	Pb^{2+}	S^{6+}	Se^{6+}	Sn^{4+}	Si^{4+}	Ti^{4+}	V^{5+}	W^{6+}	Zn^{2+}		
135	17	98	12	28	55	26	42	36	42	60		

Coordination Number = 8

Bi^{3+}	Ce^{4+}	Ca^{2+}	Ba^{2+}	Dy^{3+}	Gd^{3+}	Hf^{4+}	Ho^{3+}	In^{3+}	Na^+	Nd^{3+}	O^{2-}	Pb^{2+}
117	97	112	142	103	105	83	102	92	118	111	142	129
Rb^+	Sr^{2+}	Th^{4+}	U^{4+}	Y^{3+}	Zr^{4+}							
161	126	105	100	102	84							

Coordination Number = 12

Ba^{2+}	Ca^{2+}	La^{3+}	Pb^{2+}	Sr^{2+}
161	134	136	149	144

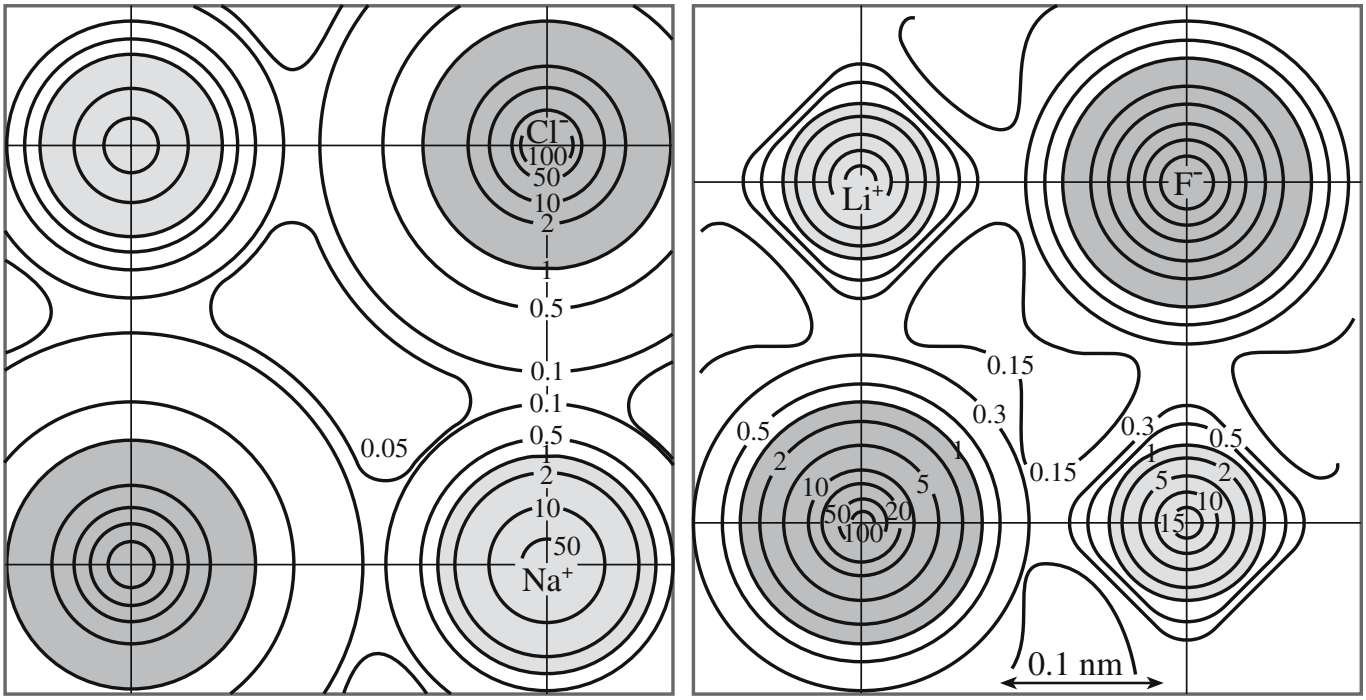

FIGURE 4.7 Electron density maps for (a) NaCl and (b) LiF.

minimum in the electron density contours between the nuclei could be taken as the radius position for each ion. The ionic radii values obtained by this method differ somewhat from those obtained by other methods and tend to make the anions smaller and the cations larger. Notice that the electron density does not go to zero in the region between nuclei even for "ionic" crystals.

4.4 COVALENT BONDING

A pure covalent bond forms when atoms that have the same electronegativity combine; the electrons are shared equally. Such a bond occurs only between identical atoms. Examples of pure covalent bonds are the C—C bond in diamond and the Si—Si bond in silicon. If the atoms have similar electronegativities, then a bond can form that has a large covalent component. The most important such bonds for ceramics are the Si—O bond found in silicates and the Al—O bond in alumina.

The bond-energy curve for a covalent bond has the same general shape as that shown in Figure 4.1a. The main difference is that we do not have the additional energy term associated with the formation of ions. The forces involved are still electrostatic:

- Attractive forces are forces between the electrons of one atom and the nucleus of the neighboring atom.
- Repulsive forces are forces between electrons on neighboring atoms.

Molecular Orbitals

One way to consider covalent bond formation is to look at what happens to the individual atomic orbitals (AOs) on adjacent atoms as they overlap at short distances to form molecular orbitals (MOs). The simplest case is that of two 1s orbitals. At relatively large separations (≥1 nm) the electron orbital on one atom is not influenced significantly by the presence of the other atom. As the two atoms approach each other the orbitals overlap and the electron density between the nuclei increases. At r_0, the individual AOs become a single MO—called a bonding MO—with the electron density concentrated between the nuclei.

A bonding MO can be described as the sum of the wave functions of the contributing AOs:

$$\Psi_{Bond} = \Psi_A + \Psi_B \tag{4.19}$$

The probability of finding an electron at a given point in the MO is proportional to Ψ^2_{Bond}:

$$(\Psi_{Bond})^2 = (\Psi_A + \Psi_B)^2 \tag{4.20}$$

Equation 4.20 is shown as a function of internuclear distance in Figure 4.8.

We can represent an MO pictorially in a manner similar to the way we do for AOs by outlining a shape that encloses most of the electron density and, consequently, is given by the molecular wave function. Figure 4.9 represents the bonding MO formed by the combination of two

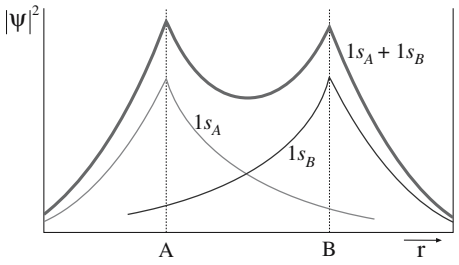

FIGURE 4.8 Distribution showing the probability of finding an electron at a given point in an MO as a function of distance.

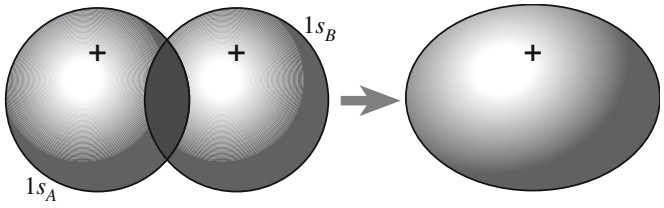

FIGURE 4.9 Pictorial representation of a bonding MO obtained by summing two AOs. In this case the example is H_2.

1s AOs. Because regions of high electron density lie between the atoms, covalent bonds are directional. The directional nature greatly influences the atomic arrangements in covalently bonded solids and their mechanical properties. Diamond, a purely covalently bonded ceramic, is the hardest known material.

We can also form an MO—called an antibonding MO—by subtracting the wave functions of the contributing orbitals:

$$\Psi_* = \Psi_A - \Psi_B \tag{4.21}$$

In the antibonding MO, illustrated in Figure 4.10, the electron density is greatly reduced in the overlap region and is zero midway between the nuclei. The antibonding MO is less stable than the isolated AOs from which it is derived and consequently is higher in energy.

MOs that are symmetrical when rotated around a line joining the nuclei are called sigma (σ) MOs. The bonding

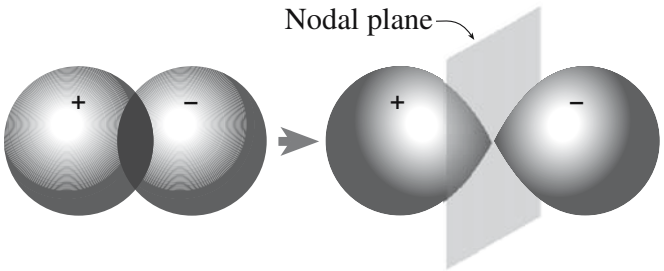

FIGURE 4.10 Pictorial representation of the formation of an antibonding MO. An appropriate example would again be H_2.

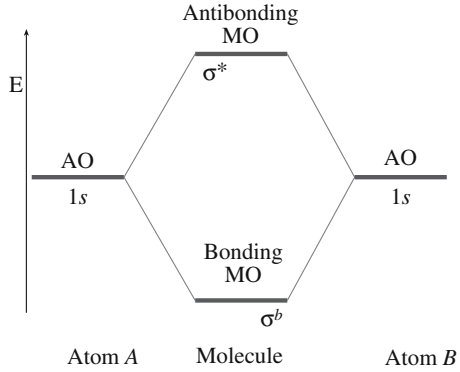

FIGURE 4.11 Energy level diagram for the H_2 MOs and the corresponding AOs.

and antibonding MOs are referred to as σ^b and σ^*, respectively. Figure 4.11 shows the relative energies of these MOs at r_0. From two 1s AOs, which have the same energy, we can construct two MOs. The bonding MO is lower in energy than the AOs and the antibonding MO is higher in energy.

We can also form MOs from the overlap of p orbitals. There are three p orbitals that are equivalent in shape and volume but point along different coordinate axes. Figure 4.12 shows six different kinds of MO formed from overlap of the p_x, p_y, and p_z orbitals.

On the convention of assigning coordinate axes: The line that connects the nuclei in a diatomic molecule is designated the *z*-axis and is thus common to both nuclei. The two sets of corresponding *x*- and *y*-axes are parallel.

The overlap of the p_z orbitals is qualitatively similar to the overlap of s orbitals and the bonding MO is designated

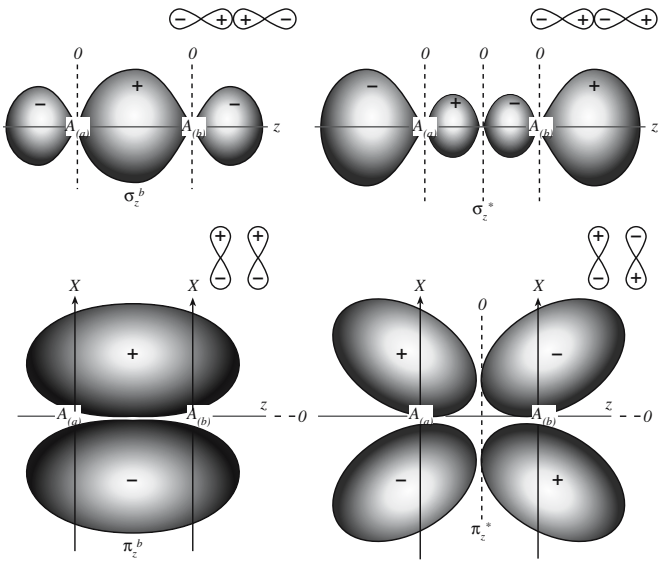

FIGURE 4.12 MOs formed from the p_z (top figure) and p_x (bottom figure) AOs. The original AOs are shown at the upper right of each MO.

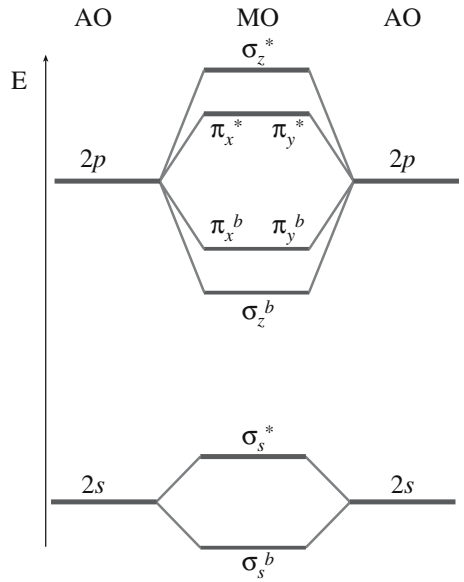

FIGURE 4.13 Energy level diagram for homonuclear diatomic molecule where there is negligible s-p hybridization.

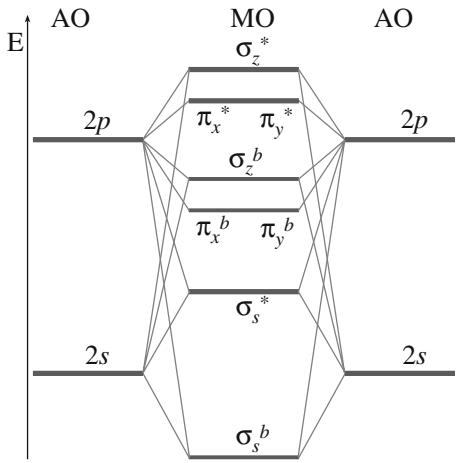

FIGURE 4.14 Energy level diagram for homonuclear diatomic molecule where s-p hybridization has occurred.

σ_z^b. The two p_x orbitals and the two p_y orbitals do not overlap along the *z*-axis, rather they overlap above and below it. This type of MO is called a π orbital. The π MOs that concentrate electron density in the region between the two nuclei are known as π bonding MOs. The combination of p_x orbitals produces a bonding MO π_x^b, while the combination of p_y orbitals produces a bonding MO π_y^b. These two MOs have the same shape and energy, but are orthogonal.

Following the convention used for the antibonding σ MOs, the π antibonding MOs are denoted by π_x^* and π_y^*. Assuming no mixing of the s and p orbitals, the relative energies of the MOs are

$$\sigma_s^b < \sigma_s^* < \sigma_z^b < \pi_x^b = \pi_y^b < \pi_x^* = \pi_y^* < \sigma_z^*$$

A diagram of these energy levels is shown in Figure 4.13. It was constructed by allowing only those interactions between those orbitals on atom A and atom B, which have the same energy. Actually interactions can occur between AOs on the *same* atom provided that the energy between the orbitals is not too large. This new arrangement of the electrons is called hybridization.

Hybridization of Atomic Orbitals

In atoms containing AOs that are close in energy different orbitals can mix to give so-called hybrid orbitals. Mixing between 1s and 2s orbitals will not occur. For example, in Na the energy difference between these orbitals is 9 MJ/mol. The energy difference between the 2s and 2p orbitals is less and varies with *Z*. In F, the energy difference between the s and p orbitals is large enough that we neglect mixing. However, in the case of elements to the left of F in the periodic table mixing between the 2s and 2p AOs is important and results in a change in the order of the levels as shown in Figure 4.14.

An sp hybrid orbital formed from one s orbital and a single p orbital is illustrated in Figure 4.15. A combination

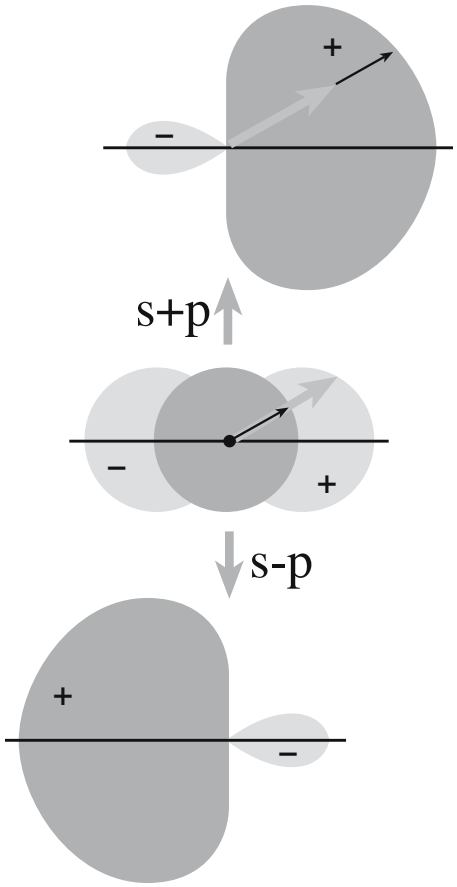

FIGURE 4.15 Two sp hybrid orbitals formed by adding and subtracting the corresponding wave functions.

of s and p orbitals causes reinforcement in the region in which the sign of the wave function is the same and cancellation where the signs are opposite.

We can represent these situations mathematically:

$$\Psi_{sp1} = \Psi_s + \Psi_p \tag{4.22}$$

$$\Psi_{sp2} = \Psi_s - \Psi_p \tag{4.23}$$

where Ψ_s and Ψ_p are the wave functions of an s and p orbital and Ψ_{sp1} and Ψ_{sp2} represent the new sp orbitals. This process is very similar to the formation of MOs. Keep in mind, however, that in the present case we are combining two or more orbitals on the same atom to form a new set of hybrid AOs.

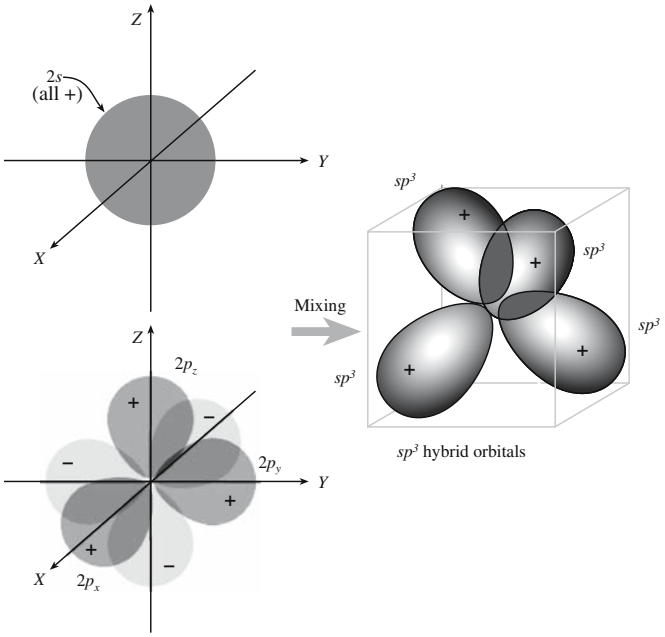

FIGURE 4.16 Formation of sp^3 hybrid orbitals.

Hybridized Orbitals in Ceramics

A very important example of hybridization occurrs between one s orbital and three p orbitals to form sp^3 hybrid orbitals. In carbon, the ground state electron configuration is $1s^2 2s^2 2p_x^1 2p_y^1$; in this state carbon would be divalent because only the unpaired electrons in the p_x and p_y orbitals are available for bonding. To form four bonds, carbon must be raised to its valence state. This requires the promotion of one of the s electrons from the 2s orbital to the formerly empty $2p_z$ orbital. The electron configuration now becomes $1s^2 2s^1 2p_x^1 2p_y^1 2p_z^1$. This promotion costs 406 kJ/mol, but is more than compensated for by the formation of two extra C–C bonds. The C–C bond energy is 348 kJ/mol.

Hybridization between the 2s, $2p_x$, $2p_y$, and $2p_z$ orbitals occurs to form four equivalent sp^3 hybrid orbitals, as shown for carbon in Figure 4.16. Each sp^3 hybrid orbital has 25% s and 75% p character. The four sp^3 orbitals are directed toward the corners of a regular tetrahedron. Thus, in diamond each carbon atom has four localized tetrahedral sp^3 hybrid orbitals. A C–C MO is formed when orbitals from neighboring carbon atoms combine. The angle between three carbon bonds is 109°28′. For covalently bonded materials that show tetrahedral coordination, sp^3 hybridization must occur.

Points to Note:

- Promotion of electrons to form an excited state can occur independently of hybridization.
- Hybridization prohibits certain configurations and allows others (C hybridizes sp^3 in diamond and sp^2 in graphite).
- The local atomic order depends upon mutual repulsion of the valence electrons and space requirements.
- The structure a material adopts is the one that has the lowest energy.

In diamond, for each tetrahedral group there are four sp^3 orbitals associated with the central carbon and one from each neighboring carbon, forming four bonds. The four electrons from the central carbon and one from each neighboring carbon are just sufficient to fill the bonding MOs. The four antibonding orbitals are empty. In diamond, the bonding and antibonding MOs are separated by a large energy as shown in Figure 4.17. This energy gap is the reason diamond is an electrical insulator at room temperature. (We will discuss the energy gap again in Section 4.8 and Chapter 30.)

Several other important ceramic materials in which the bonding is predominantly covalent have tetrahedral

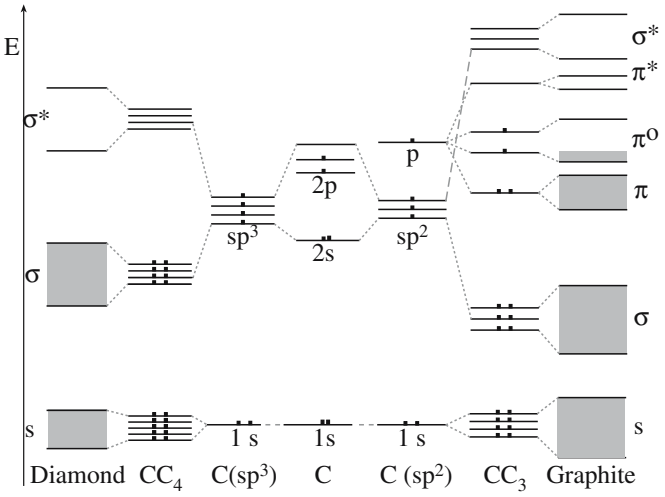

FIGURE 4.17 Energy level diagram for diamond and graphite.

coordination of nearest-neighbor atoms, for example, silicon carbide (SiC) and aluminum nitride (AlN). In these materials sp^3 hybridization has occurred but, because of the different electronegativities of the constituent atoms, the electron density will not be symmetrical in a plane drawn between the atoms. The crystal structure of these materials is described in Chapter 6.

In graphite, the carbon atoms are in a trigonal planar arrangement with each carbon bonded to three nearest neighbors. The carbon is sp^2 hybridized. Hybridization occurs between the C 2s orbital and the $2p_x$ and $2p_y$ orbitals producing three hybrid orbitals lying in a plane at 120° to each other. Overlap of the sp^2 hybrid orbitals to produce localized bonds between carbon atoms results in a hexagonal network.

The strong bonding between carbon atoms causes overlap of adjacent $2p_z$ orbitals, which are aligned perpendicular to the plane of the hybrid orbitals. This overlap is termed π-type overlap. Since the $2p_z$ orbital is half-filled the π band will only be half full as shown in Figure 4.17. This half-filled band is why graphite has a high electrical conductivity.

In hexagonal boron nitride (h-BN), which has a structure similar to graphite, the bonding between the B and N atoms is predominantly covalent and the trigonal planar structure in the layers is a result of sp^2 hybridization of the atomic orbitals of the B and N atoms. The ground state electronic configuration of B is $1s^2 2s^2 2p_x^1$; one 2s electron is promoted to the $2p_y$ orbital giving the electron configuration $1s^2 2s^1 2p_x^1 2p_y^1$. The unfilled 2s and 2p orbitals hybridize to form three equivalent sp^2 hybrid orbitals. Nitrogen has the electronic configuration $1s^2 2s^2 2p_x p_y p_z$. Promotion of one of the 2s electrons gives the following electron configuration to the atom $1s^2 2s 2p_x 2p_y 2p_z^2$. The three half-filled orbitals combine to give three sp^2 hybrids in the *xy* plane.

The spatial arrangement of atoms around each N atom is the same as that around each B atom. Structurally there are many similarities between h-BN and graphite and both can be converted under high temperature and pressure into a cubic form. The crystal structures of cubic boron nitride (c-BN) and diamond are similar. However, unlike graphite, h-BN is an electrical insulator. The reason for this difference is that the p_z orbitals in h-BN, which lie perpendicular to the plane of the network, are either empty in the case of B or filled in the case of N. Because the energies of the p orbitals on B and N are quite different, there is little interaction, with no delocalization as was the case in graphite.

- h-BN is a white or colorless insulator.
- Graphite is a shiny black or gray electrical conductor.

Hybridization can also involve d orbitals (for atoms with $Z > 21$). The shapes produced are more complicated than those for hybridization only between s and p orbitals. Table 4.7 lists some hybrid orbitals containing s, p, and d orbitals and these are illustrated in Figure 4.18. Hybridization involving s, p, and d orbitals occurs in MoS_2. Mo ($Z = 42$) has the electron configuration [Kr] $4d^5 5s^1$. One of the 4d electrons is promoted into the empty p_x orbital to give the following electron configuration: [Kr] $4d^4 5s^1 5p_x^1$. Hybridization occurs to produce d^4sp hybrid orbitals on each Mo atom, resulting in trigonal prismatic coordination with each Mo being surrounded by six sulfur atoms.

For most ceramic materials we will not need to consider hybridization involving d orbitals. However, even when they are not involved in bonding the d orbitals can be extremely important in determining the properties of materials (particularly magnetism).

TABLE 4.7 Orbital Geometries for Hybridization

Number of bonds	*Representation*	*Shape*	*Example*
2	sp	Linear	BeH_2, $HgCl_2$
3	sp^2	Trigonal	B_2O_3, BN, graphite
4	sp^3, dsp^2	Tetrahedral Square planar	SiO_2, diamond $AuBr_4$
5	dsp^3, d^3sp, d^2sp^2, d^4s	Trigonal bipyramid Square pyramid	PCl_5 IF_5
6	d^2sp^3, d^4sp	Octahedral Trigonal prism	MoO_3 MoS_6 in MoS_2
8	d^4sp^3, d^5p^3	Dodecahedral Square antiprism	— —

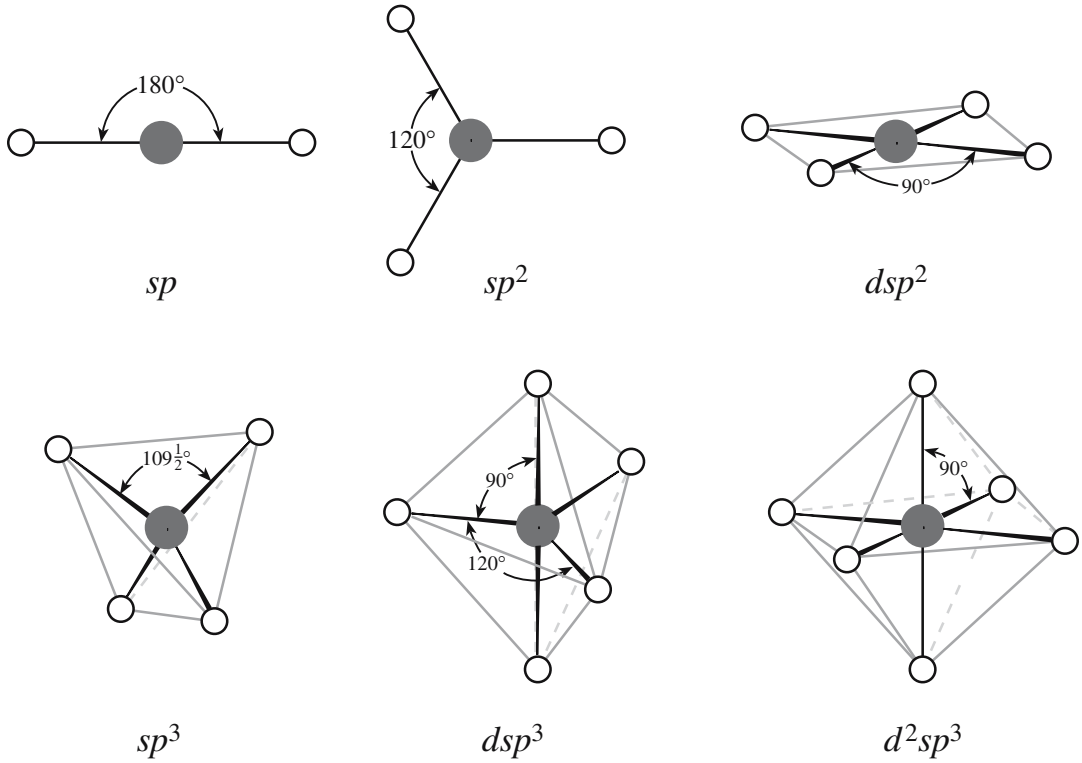

FIGURE 4.18 Geometric arrangements of some hybrid orbitals involving s, p, and d AOs.

4.5 METALLIC BONDING IN CERAMICS

Metallic bonding is the primary bond in metals and can be thought of as an electrostatic interaction between the delocalized valence electrons and the positively charged ion cores. It is the delocalized electron gas that gives rise to many of the characteristic properties of metals such as high electrical and high thermal conductivities. Metallic bonds do not require a balance of the electric charge between the elements; the electrostatic equilibrium is between the metal ions and the electron gas. For this reason different elements can mix in metallic alloys in arbitrary ratios.

Metallic bonding is traditionally neglected because of the definition of a ceramic. However, some compounds that are thought of as ceramics can, under certain conditions, show metallic behavior. Others can even be superconducting. (Superconductivity is a property associated with both metals and ceramics.) So it helps to keep a more open view of ceramics.

In addition to bonds showing mixed covalent and ionic character, the bonding in some ceramics shows partial metallic character. Transition metal carbides (e.g., TiC and Mo_2C) and nitrides (e.g., TiN and NbN) have properties that suggest both metallic and covalent bonding occurs in the crystal.

- TiN is gold in color and is an electrical conductor.
- TiN has a very high melting point (2949°C) and is brittle at 25°C.

The former suggests it is a metal; the latter properties are associated with ceramics. The bonding in transition metal carbides and nitrides is very complex. It consists of a combination of metal-to-metal and metal-to-nonmetal interactions and involves simultaneous contributions of metallic, covalent, and ionic bonding.

The exact details of the bonding mechanisms in these ceramics are still controversial, and several different approaches to explain the wide range of observed properties have been suggested. One common feature to all the proposed mechanisms is that of orbital hybridization. Hybridization of the s, p, and d orbitals of the transition metal as well as hybridization of the s and p orbitals of the nonmetal has been proposed.

The transition metal borides also show characteristics of covalent and metallic materials. The bonding in the borides is also complicated by the fact that there are interactions between the B atoms to form chains, layers, or three-dimensional networks. In the carbides and nitrides there are no C–C or N–N interactions. Despite these complexities we can still use some of the same approaches that we use for simple oxides (Chapter 6) to predict the crystal

structure of these ceramics. The point to remember is that the bonding in ceramics is usually mixed and is occasionally very complex. Many of the new ceramics are interesting because of their special properties and these often occur because the bonding is mixed.

4.6 MIXED BONDING

From the preceding sections it should be clear that in ceramics we do not usually have pure ionic bonds or pure covalent bonds but rather a mixture of two, or more, different types of bonding. Even so it is still often convenient and a frequent practice to call predominantly ionically bonded ceramics "ionic ceramics" and predominantly covalently bonded ceramics "covalent ceramics."

From the series of electronegativity values we can form some general rules about bonding.

- Two atoms of similar electronegativity will from either a metallic bond or a covalent bond, according to whether they can release or accept electrons, respectively.
- When the electronegativities differ the bond is partially ionic.

The ionic character of a bond increases with the difference in electronegativity of the two atoms as shown by Eq. 4.24:

$$\text{Fraction of ionic character} = 1 - \exp[-0.25\,(X_M - X_X)^2] \tag{4.24}$$

X_M and X_X represent the electronegativities of M and X (keeping the cation/anion labeling). Using Eq. 4.26 and electronegativity values in Table 3.6 we can see that B_4C, SiC, and BN are highly covalent (6%, 12%, and 22% ionic character, respectively). Oxides of the alkali metals and alkaline-earth metals are predominantly ionic. The metal–oxygen bond in MgO has 73% ionic character and 82% ionic character in BaO. Some important ceramics fall in between these limits, for example, GaN (38% ionic character), SiO_2 (51% ionic character), ZnO (59% ionic character), and Al_2O_3 (63% ionic character). In bonding that shows mixed ionic-covalent characteristics, the electrons are located closer to the electronegative atom (compare the electron densities around the Li^+ and F^- ions in Figure 4.19).

Since the covalent bond is directional, while the ionic bond is not, the degree of directionality changes with bond character. Such changes can have a marked influence on crystal structure. Both ionic and covalent bonds can be very strong, but since covalent bonds are directional, covalent materials respond differently to deformation. The fraction of covalent character can thus influence the mechanical properties of the ceramic.

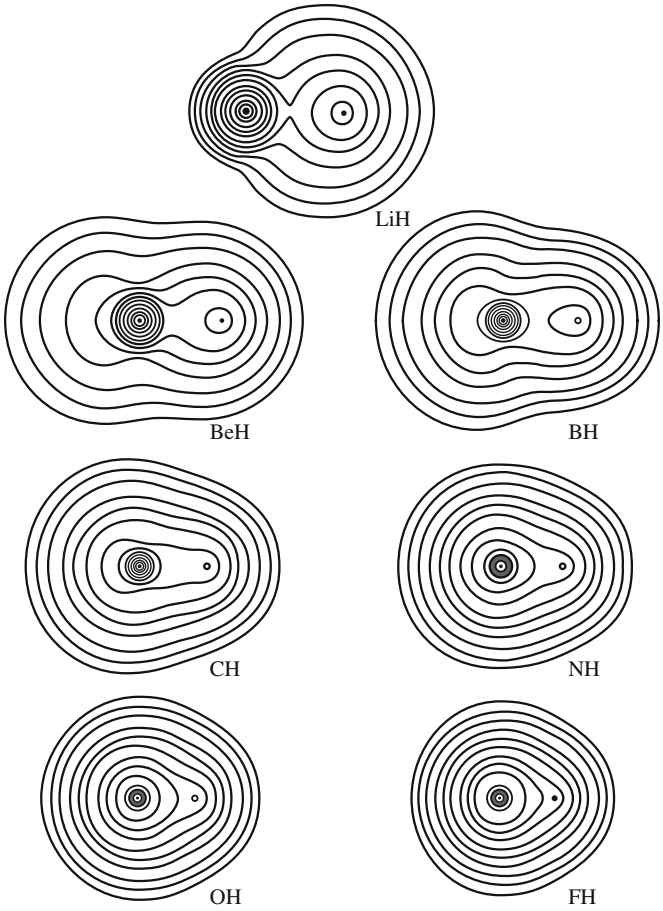

FIGURE 4.19 Contours of constant electron density in the first row hydrides.

4.7 SECONDARY BONDING

Secondary bonds are so called because the compound involved invariably also has ionic or covalent bonding. Secondary bonds are generally much weaker than primary bonds, although they can be critical in determining both the existence of a particular crystal structure and the properties of a material.

van der Waals Bonding

The origin of van der Waals bonding (known also as the London interaction) is weak electrostatic attraction between closely spaced neutral atoms and molecules. The explanation for this universally attractive force is that even a neutral atom has a charge distribution that fluctuates very rapidly. When two atoms are brought together the fluctuations in one can induce a field around the other and this coupling results in the attractive force. Although van der Waals bonding is present in all crystalline solids it is important only when not overwhelmed by strong bonding forces.

The energy of a crystal bound by van der Waals forces can be expressed by the Lennard–Jones potential with two constants, A_{LJ} and B_{LJ}

$$E = -\frac{A_{LJ}}{r^6} + \frac{B_{LJ}}{r^{12}} \tag{4.25}$$

Again, the potential is empirical: it provides a good fit to the experimental data. Both the repulsive and attractive terms decrease rapidly with increasing r. The attractive van der Waals forces are proportional to $1/r^7$ and are, therefore, of much shorter range than the ionic (Coulombic) forces, which are proportional to $1/r^2$.

In ceramics, van der Waals bonding is important in layered structures. In pyrophyllite, a layered silicate, van der Waals bonds between the oxygen ions in adjacent layers allow easy slip parallel to the layers. In the mineral talc, van der Waals bonds between the layers are even weaker than in pyrophyllite. You can cleave talc with your fingernail.

In graphite and hexagonal boron nitride there is strong covalent bonding within each layer. Between the layers the bonding is van der Waals. These materials show highly anisotropic properties, for example, in their mechanical strength. Little effort is required to separate the sheets, but much more effort is required to break them.

MoS_2 has a structure built of MoS_6 units where each Mo is surrounded by six S atoms. The layers are joined by van der Waals bonds between the S atoms and can slip over one another easily so that MoS_2 has mechanical properties that are similar to those of graphite.

Hamaker Constant

van der Waals interactions are just as important at the macroscopic level, where they can influence behavior such as wetting and fracture, as they are at the atomic and molecular level. The interaction energies between different macroscopic geometries can be described in terms of the Hamaker constant, $\mathcal{A}$ as shown in Figure 4.20.

$$\mathcal{A} = \pi^2 A_{LJ} \rho_1 \rho_2 \tag{4.26}$$

where A_{LJ} is the coefficient in Eq. 4.25 and ρ_1 and ρ_2 are the number of atoms per unit volume in the two bodies. Typical values for Hamaker constants are about 10^{-19} J for interactions across vacuum (or air); values for some ceramics are listed in Table 4.8. We can use these values to estimate the strength of the van der Waals interactions between, for example, two spherical particles using the equations in Figure 4.20. Remember that the forces are obtained by differentiating the energies with respect to distance.

TYPICAL VALUES IN CALCULATING $\mathcal{A}$

$A_{LJ} \sim 10^{-77}\,\text{J m}^6$
$\rho \sim 3 \times 10^{28}\,\text{m}^{-3}$ (for $r \sim 0.2\,\text{nm}$)

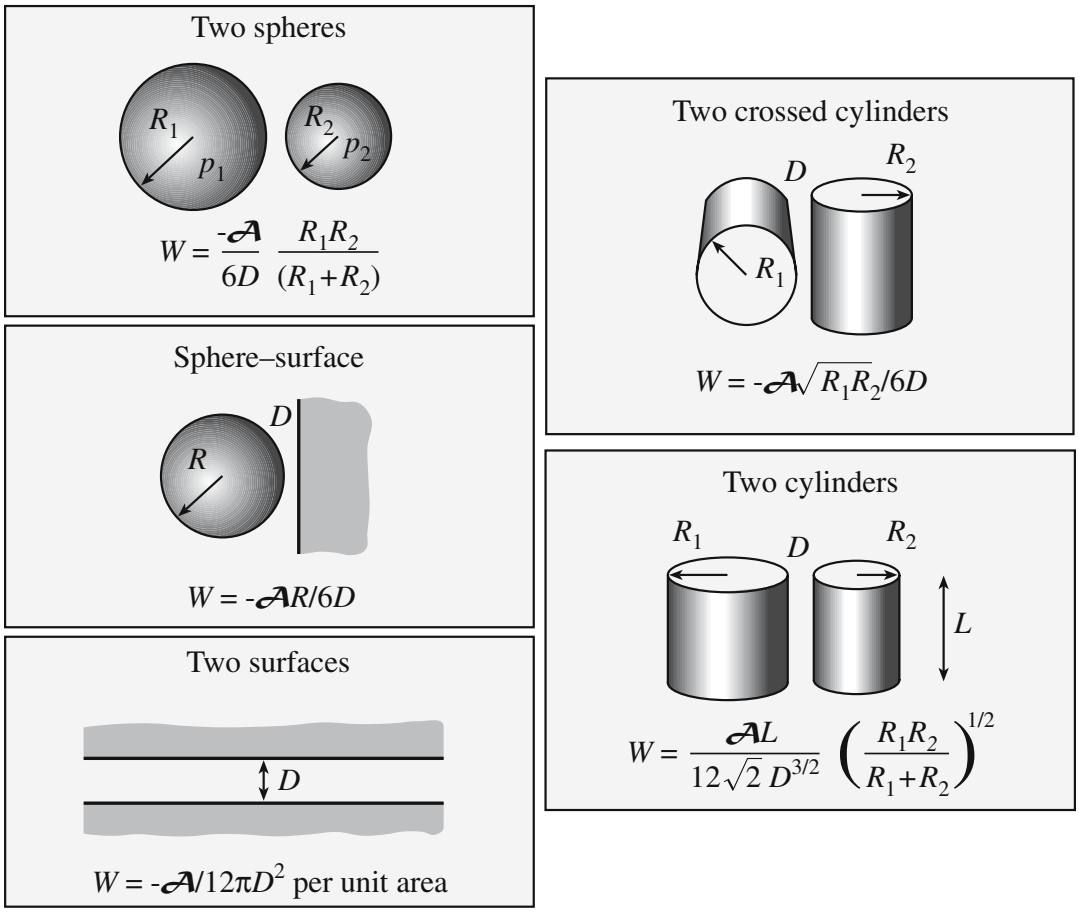

FIGURE 4.20 Interaction energies for macroscopic geometries. The key is the Hamaker constant, $\mathcal{A}$.

TABLE 4.8 Hamaker Constant

Material	$\mathcal{A}$ *(zJ)*
Al_2O_3	140
Fe_3O_4	210
ZrO_2	270
TiO_2	430
SiC	440
Fused quartz	63
Mica	100
CaF_2	70

TABLE 4.9 Hamaker Constants for Fused Quartz Interacting with Air across Another Medium

Medium	$\mathcal{A}$ *(zJ)*
Water	−8.7
Octane	−7
Tetradecane	−4

Things, as you might expect, are actually a little more complicated than Eq. 4.26 implies. We need, as in the calculation of the Madelung constant, to consider the influence of neighboring atoms on the interaction between any pair of atoms. An alternative method developed by Lifshitz (1956) for determining $\mathcal{A}$ uses bulk properties of a material such as dielectric constants and refractive indices. The values given in Table 4.8 were calculated using this approach. In general, materials with high dielectric constants and refractive indices have higher values of $\mathcal{A}$. If the interactions occur across a medium then the value and sign of $\mathcal{A}$ may change as shown in Table 4.9.

Hydrogen Bonding

Hydrogen bonds are usually stronger than van der Waals bonds but still considerably weaker than primary bonds. Hydrogen bonds occur when a hydrogen atom that is in an ordinary covalent bond joins another, usually highly electronegative atom. The classic example in which such bonds are important is, of course, water. The H–O bonds in the H_2O molecule are fully saturated, yet the bonds between the molecules can be so strong that ice forms with a well-defined crystal lattice.

In kaolinite, hydrogen bonds can form between basal oxygen atoms of one plane and the upper hydroxyl groups of the next. The weak hydrogen bonding between each octahedral–tetrahedral double layer makes the materials very anisotropic. Layers easily slip over one another giving the material a greasy feel and making it excellent for molding, particularly when water is present.

4.8 ELECTRON ENERGY BANDS IN CERAMICS

The energy levels for electrons in a single isolated atom are highly discrete and given by Box 3.6 in Chapter 3. When a number of atoms are brought together to form a solid the Pauli exclusion principle does not allow any two electrons to have the same set of four quantum numbers. The energies that were identical in the isolated atoms shift relative to one another in the formation of a molecule and subsequently a solid. The sharply defined electronic energy levels broaden into an allowed band of energies when a large number of atoms are brought together to form a solid. We illustrated how this happens in diamond and graphite in Figure 4.17.

If we think of a solid as just a very large molecule then we can view the formation of electron energy bands as arising from a combination of a large number of MOs. As the molecule becomes larger, the number of MOs increases and they become more closely spaced in energy. In a solid the number of MOs is so large that we can regard them simply as a continuous band of energy levels.

If we consider the case of diamond, the highest occupied band, referred to by chemists as the highest occupied molecular orbital (HOMO), is σ^b. The lowest unoccupied band, referred to as the lowest unoccupied molecular orbital (LUMO), is the σ^*. Although the bands themselves are important, the most significant aspect of these diagrams is the energy gap between bands. Knowledge of the band gap energy, which is related to chemical bonding, will allow us to draw important conclusions about the electrical conductivity of a material.

The effect of distance on the formation of energy bands is illustrated in Figure 4.21. The closer the atoms are together the more marked is the shift in available energy states. The higher energy states broaden first. Broadening of the lower energy states, which are closer to the nucleus, is less marked.

In materials science we usually define the highest filled electron energy band when the material is in its ground state as the valence band. The lowest energy band containing unoccupied states when the material is in its ground state is the conduction band. At absolute zero the electrons occupy the lowest available energy states; the energy of the highest occupied state is the Fermi energy, E_F. This energy level separates the occupied from the unoccupied electron levels only when the electron configuration is in its ground state (i.e., at 0 K).

A solid behaves as an insulator if the allowed energy bands are either filled or empty, for then no electrons can move in an

DENSITY OF STATES

$$N(E) = \frac{\pi}{4}\left(\frac{8m}{h^2}\right)^{\frac{3}{2}} E^{\frac{1}{2}}$$

Fermi–Dirac distribution:

$$P(E) = \frac{1}{\exp[(E - E_F)/kT] + 1}$$

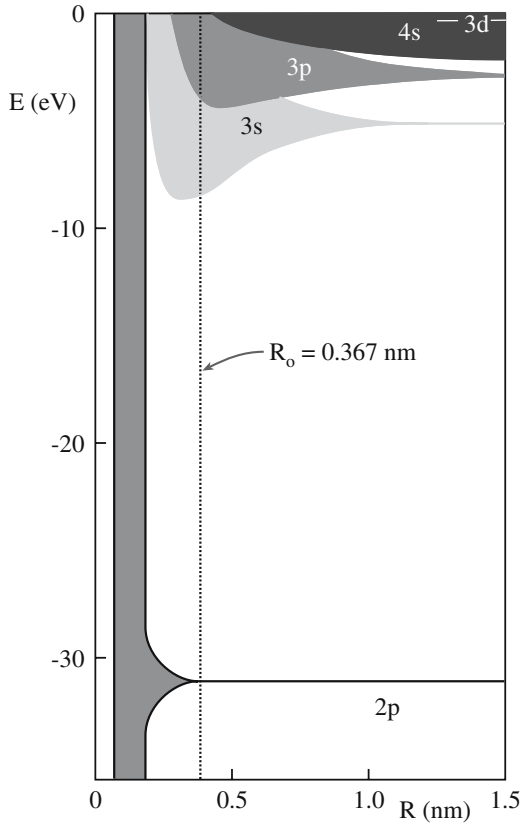

FIGURE 4.21 Formation of electron "bands" as the interatomic spacing is reduced.

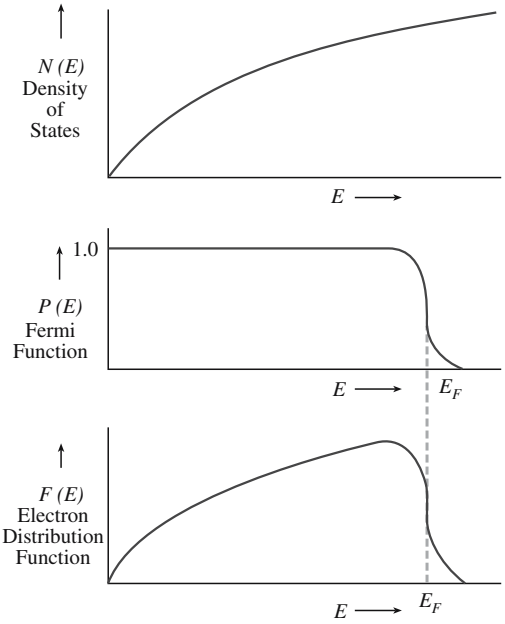

FIGURE 4.22 Electron distribution functions.

electric field. Metals always have a partially filled valence band; the Fermi energy is in the middle of the band and this makes the metals electrical conductors. In semiconductors and insulators we always have completely filled or completely empty electron bands; the Fermi energy lies between the bands, and consequently they are not good electrical conductors at ambient temperatures.

Classically, the valence and conduction bands in ceramics are well separated, so they are insulators. In perfect insulators the gap between bands is so large that thermal excitation is insufficient to change the electron energy states, and at all temperatures the conduction band contains essentially zero electrons and the next lower band of energy is completely full, with no vacant states.

In models of electrons in solids we usually introduce two functions:

- Density of states, $N(E)$, defines the number of energy states available to electrons. There are no available energy states in the band gap and so $N(E)$ is zero in this region.
- Fermi function, $P(E)$, defines the probability of finding an electron at a particular energy state.

These functions are shown graphically in Figure 4.22 together with the electron distribution function $F(E)$:

$$F(E) = 2N(E)P(E) \tag{4.27}$$

In this book we will primarily represent the energy levels of a solid as the familiar and simple block diagrams showing the band gaps. This approach is straightforward, but the question that is often asked is what are we plotting on the x-axis? A more satisfactory form is illustrated in Figure 4.23 where we plot the density of states versus energy. Either description allows the prediction of the electrical properties of a material based on the size of E_g. So we can determine whether a material will behave as a conductor or an insulator.

It is possible to convert an insulator to a metal under very high pressures as a result of the broadening of the energy bands that occurs when the atomic cores are moved closer together as shown in Figure 4.24. If we assume that the Fermi level does not change, then the material will undergo a transition from insulator to metal at the point at which the valence and conduction bands begin to overlap. Very high pressures are required to cause this type of transition. For example, germanium is usually a

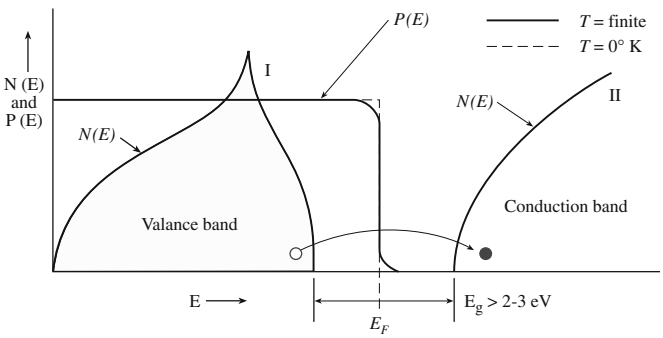

FIGURE 4.23 Plot of the density of states function and Fermi function versus energy.

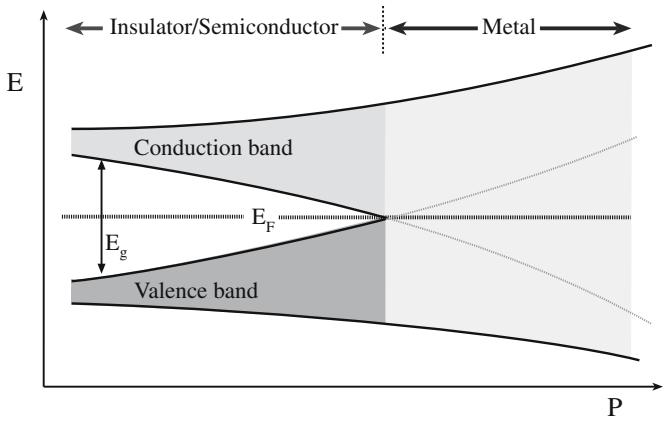

FIGURE 4.24 Plot of energy versus pressure illustrating how an insulator-to-metal transition can occur at high pressures.

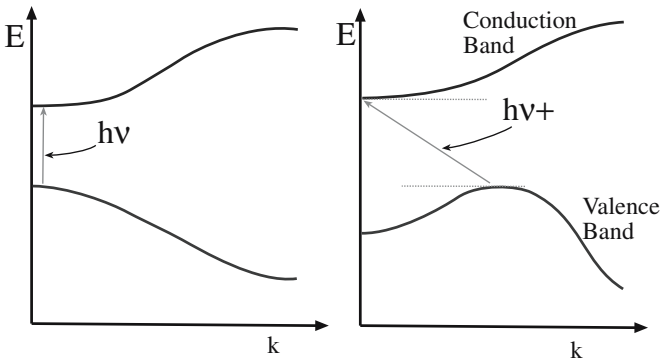

FIGURE 4.25 Illustration of direct and indirect band gap transitions. Energy is plotted versus wave vector.

TABLE 4.10 Critical Pressure for Metal–Insulator Transformation at 300 K

Material	*P (GPa)*
C	168
BN	211
SiC	64
AlN	90
GaN	87

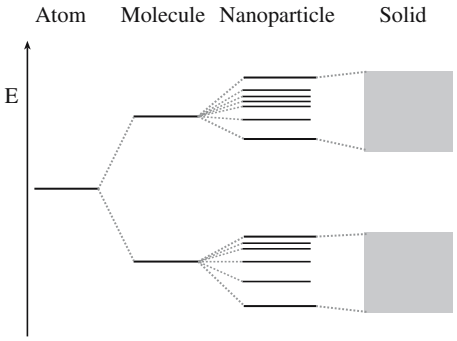

FIGURE 4.26 Illustration of how the energy band gap arises in a nanoparticle.

semiconductor with a band gap of 0.7 eV. It becomes a metal under a pressure of 12 GPa. Examples of critical pressures for insulator–metal transitions at 300 K in some ceramics are given in Table 4.10.

To understand some of the optical properties of ceramics and why certain materials may be favored for solar cell or laser applications, we need to know whether the band gap is direct or indirect. The two situations are illustrated in Figure 4.25. The electrons in a band have both energy and momentum (they are not bound) expressed as a wave vector, **k**, with units of reciprocal length (usually cm^{-1}). Energy diagrams can be plotted for different wave vectors.

In direct band gap materials the top of the valence band and the bottom of the conduction band are located at the same point in **k** space. This is not the case for an indirect band gap. It is direct band gap materials that are of most interest for optoelectronic applications.

The probability of electronic transitions across the band gap is higher in materials with a direct band gap and this results in higher efficiency in devices such as lasers and LEDs.

Before we leave this chapter a word must be given about nanomaterials. The value of E_g for nano-sized crystals is often significantly larger than for the bulk form of the material. This is associated with how the bands broaden as the number of atoms in the solid increases as illustrated in Figure 4.26.

As an example, bulk silicon has $E_g = 1.1$ eV. For nanocrystalline silicon E_g varies with the size of the crystals and for sizes less than 2 nm $E_g > 2$ eV.

CHAPTER SUMMARY

This chapter was a review of things that you already knew. There are three types of primary bonds that are used to hold atoms together. In introductory materials science classes we tend to think of each type of bond as being a distinct form, with materials adopting one type or another. At a qualitative level this approach might work, and in the cases of many metals, semiconductors, and polymers it is usually quite close to the actual situation we encounter. However, in ceramics almost every bond has a mixture of covalent, ionic, and, in some cases, metallic character. The type of interatomic bond affects the crystal structure that a material adopts. The influence of mixed bonding can mean that the type of structure predicted, based

on either purely ionic or purely covalent bonding, is incorrect. The role of hybridization, or mixing, of atomic orbitals is very important in ceramics, which are predominantly covalently bonded. For example, the tetrahedral coordination of carbon atoms in diamond requires the sp^3 hybridization.

We discussed the concept of energy bands here, both in terms of the broadening of electron energy states and also from the MO approach. Knowledge of electron energy band diagrams is essential in understanding the electrical properties of materials. The most important feature of the energy band diagram is the band gap. There are no available states in this region.

Secondary bonding is also important in many ceramics. The most familiar properties of graphite, hexagonal-BN, and clay minerals are determined by the presence of weak secondary bonds.

PEOPLE IN HISTORY

Born, Max was born in Breslau in 1882. He graduated from the University of Göttingen in 1907 where he worked on the stability of elastic wires and tapes. During the World War I he had to join the German Armed Forces where in a scientific office he worked on the theory of sound ranging. After the war he was appointed Professor at the University of Frankfurt-on-Main. In 1933 he was forced to emigrate from Germany and came first to Cambridge University in England, then to the Indian Institute of Science in Bangalore, and finally to the University of Edinburgh in Scotland, where he worked until his retirement in 1953. He won the 1954 Nobel Prize in Physics and died in 1970.

Haber, Fritz was born in Breslau, Germany in 1868. He completed his studies at the University of Heidelberg, the University of Berlin, and the Technical School at Charlottenberg. The Haber process for the synthesis of ammonia was patented in 1908 and by 1914 the process was into quantity production. Ammonia was important in Germany's war efforts as a source of nitric acid, which is essential for the manufacture of explosives. It is clear that this prolonged the war. Haber was given the 1918 Nobel Prize in Chemistry (actually awarded in 1919) for his work on nitrogen fixation. In 1933 Haber resigned from his post as Director of the Institute for Physical and Electrochemistry at Berlin-Dahlem. He died in exile in Switzerland in 1934.

Madelung, Erwin was born in 1881 in Bonn, Germany. From 1921 to 1949 he was Professor of Theoretical Physics at Frankfurt University. He died in 1972.

van der Waals, Johannes Diderik was a Dutch physicist, born in Leyde in 1837; he died in Amsterdam in 1923. He was awarded the Nobel Prize for physics in 1910 for his work on the equation of state for gases and liquids.

Young, Thomas was born in 1773. His accomplishments include his introduction of the Modulus of Elasticity. He is best known for his work in optics. He died in 1829.

GENERAL REFERENCES

Huheey, J.E. (1993) *Inorganic Chemistry: Principles of Structure and Reactivity*, 4th edition, Harper & Row, London. If the different interactions are not familiar to you from introductory chemistry or materials science classes, this text covers the material in some detail.

Kittel, C. (2004) *Introduction to Solid State Physics*, 8th edition, Wiley, New York. A more rigorous and mathematical treatment of energy bands than we give in this chapter.

Pauling, L. (1960) *The Nature of the Chemical Bond*, Cornell University Press, Ithaca, NY. Often referenced and well worth seeing.

SPECIFIC REFERENCES

Born, M. (1919) "A thermo-chemical application of the lattice theory," *Verhandl. Deut. Phys. Ges.* **21**, 13.

Born, M. and Mayer, J.E. (1932) "Lattice theory of ionic crystals," *Z. Phys.* **75**, 1.

Chase, M.W., Jr. (1998) *NIST-JANAF Thermochemical Tables*, 4th edition, American Chemical Society, Washington D.C.; American Institute of Physics for the National Institute of Standards and Technology, New York.

Haber, F. (1919) "Theory of the heat of reaction," *Verhandl. Deut. Phys. Ges.* **21**, 750.

Hamaker, H.C. (1937) "London-van der Waals attraction between spherical particles," *Physica* **4**, 1058. The original.

Johnson, D.A. (1982) *Some Thermodynamic Aspects of Inorganic Chemistry*, 2nd edition, Cambridge University Press, Cambridge, UK.

Kubaschewski, O., Alcock, C.B., and Spencer, P.J. (1993) *Materials Thermochemistry*, 6th edition, Elsevier, Oxford, UK.

Lande, A. (1920) "Size of atoms," *Z. Phys.* **1**, 191.

Lifshitz, E.M. (1956) "The theory of molecular attractive forces between solids," *Soviet Phys. JETP–USSR* **2**, 73.
Madelung, E. (1918) "The electric field in systems of regularly arranged point charges," *Phys. Z.* **19**, 524.
Shannon, R.D. and Prewitt, C.T. (1969) "Effective ionic radii in oxides and fluorides," *Acta Crystallogr* **B25**, 925. Gives the alternatives to Pauling's radii.
Shannon, R.D. (1976) "Revised effective ionic radii and systematic studies of interatomic distances in halides and chalcogenides," *Acta Crystallogr.* **A32**, 751.
van Vechten, J.A. (1973) "Quantum dielectric theory of electronegativity in covalent systems. III. Pressure-temperature phase diagrams, heats of mixing, and distribution coefficients," *Phys. Rev.* **B7**, 1479.

WWW

http://www.lrsm.upenn.edu/~frenchrh/hamaker_software.htm. Roger French's site for calculating the Hamaker constant.
www.deconvolution.com/Overview/170.htm. More on Hamaker.

EXERCISES

4.1 By considering the hybridization of orbitals in diamond explain why it is (a) an electrical insulator at room temperature and (b) extremely hard.

4.2 Why are covalently bonded materials in general less dense than metallically or ionically bonded ones?

4.3 Calculate the force of attraction between a Na^+ and a Cl^- ion the centers of which are separated by 1.5 nm.

4.4 Calculate Born–Landé lattice energies of the following compounds: NaCl, KCl, and CsCl. Compare the values you obtain to those given in Table 4.5 and discuss any differences.

4.5 Sketch bond-energy curves for two ceramics, one with a high Young's modulus and one with a low Young's modulus.

4.6 Rank the following ceramics in terms of increasing fraction of ionic character in their bonds: SiC, AlN, Si_3N_4, B_4C, GaN, Al_2O_3, and SiO_2.

4.7 Sketch a bond-energy curve for two atoms held together by van der Waals forces. Describe how this curve differs from the one shown in Figure 4.1, which is for ionic bonding.

4.8 What do we mean by the term "insulator–metal transition." Are there any practical applications for such a transition?

4.9 Estimate the force of adhesion between two spherical Al_2O_3 particles of radius 1 mm separated by a distance of 10 nm. How does the force change as the separation increases?

4.10 Estimate the surface energy of Al_2O_3. Assume that for two surfaces in contact $D \sim 0.2$ nm.